

A Direct View on Li-Ion Transport and Li-Metal Plating in Inorganic and Hybrid Solid-State Electrolytes

Liu, Ming; Ganapathy, Swapna; Wagemaker, Marnix

DOI

[10.1021/acs.accounts.1c00618](https://doi.org/10.1021/acs.accounts.1c00618)

Publication date

2021

Document Version

Final published version

Published in

Accounts of Chemical Research

Citation (APA)

Liu, M., Ganapathy, S., & Wagemaker, M. (2021). A Direct View on Li-Ion Transport and Li-Metal Plating in Inorganic and Hybrid Solid-State Electrolytes. *Accounts of Chemical Research*, 55(3), 333-344. <https://doi.org/10.1021/acs.accounts.1c00618>

Important note

To cite this publication, please use the final published version (if applicable). Please check the document version above.

Copyright

Other than for strictly personal use, it is not permitted to download, forward or distribute the text or part of it, without the consent of the author(s) and/or copyright holder(s), unless the work is under an open content license such as Creative Commons.

Takedown policy

Please contact us and provide details if you believe this document breaches copyrights. We will remove access to the work immediately and investigate your claim.

A Direct View on Li-Ion Transport and Li-Metal Plating in Inorganic and Hybrid Solid-State Electrolytes

Ming Liu,* Swapna Ganapathy, and Marnix Wagemaker*



Cite This: *Acc. Chem. Res.* 2022, 55, 333–344



Read Online

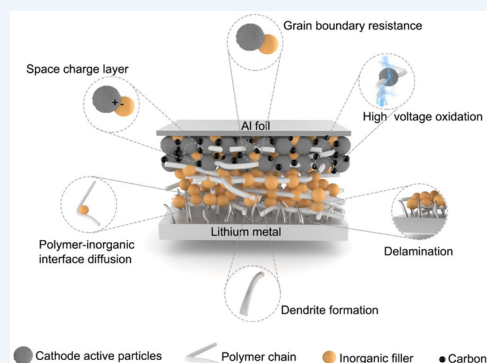
ACCESS |

Metrics & More

Article Recommendations

CONSPPECTUS: Driven by the intrinsic safety and potential to achieve higher energy densities, solid-state Li-metal batteries are intensively researched. The ideal solid electrolyte should possess a high conductivity, should have electrochemical stability both toward the Li-metal anode and to high voltage cathodes, should suppress dendrites, should provide flexibility to deal with the volumetric changes of the electrodes, and should be easy to process. This challenging combination is to date not fulfilled by any solid electrolyte, be it organic, inorganic, or even a hybrid of the two. Pushing the development of solid electrolytes toward reversible room temperature operation when used in tandem with Li-metal anodes demands an understanding of critical processes that determine the properties of the solid electrolyte. These include the complex Li-ion transport as well as the Li-metal plating processes. This already presents the first experimental hurdle as the ability to directly and noninvasively monitor the Li-ion kinetics, Li densities, and Li chemistries, under in/situ or operando, is not trivial.

The scope of this Account is the investigation and improvement of solid electrolytes, with the emphasis on the possibilities offered by solid-state NMR and neutron depth profiling as direct probes for the study of critical processes that involve Li ions and Li metal. Solid-state NMR allows us to unravel the complex interface chemical environment and the diffusion processes both in the bulk solid electrolyte and in the interface environment. These studies shed light on the role of interface composition, wetting and space-charge layers, on the macroscopic battery performance. Another technique that enables probing Li directly is operando neutron depth profiling, which allows us to determine the Li density as a function of depth. It provides a noninvasive and effectively nondestructive tool to examine delamination, irreversible reactions and dendrite formation during plating/stripping. Results demonstrate that it is very challenging to maintain the contact between Li metal and the SE during cycling, especially for the “anode-less” or “anode-free” configuration under low-pressure conditions. A perspective is provided on the potential improvement of the Li-ion transport, dendrite suppression, and preventing Li-metal-solid-electrolyte delamination as well as on the potential role of solid-state NMR and NDP techniques to guide these developments.



KEY REFERENCES

Liu, M.; Cheng, Z.; Ganapathy, S.; Wang, C.; Haverkate, A. L.; Tufodziecki, M.; Unnikrishnan, S.; Wagemaker, M. Tandem Interface and Bulk Li-Ion Transport in a Hybrid Solid Electrolytes with Microsized Active Filler. *ACS Energy Lett.* 2019, 4, 2336–2342.¹ It is demonstrated that the organic and inorganic interface environment plays a key role in utilizing the high conductivity of the inorganic particles.

Liu, M.; Wang, C.; Cheng, Z.; Ganapathy, S.; Haverkate, L. A.; Unnikrishnan, S.; Wagemaker, M. Controlling the Li-metal growth to enable low Li-metal excess all solid state Li-metal batteries. *ACS Mater. Lett.* 2020, 2, 665–670.² A 100 nm thin layer of ZnO is deposited on the copper current collector with atomic layer deposition (ALD) enabling controllable Li morphology and an “anode-less” solid-state battery directly examined by operando neutron depth profiling.

Cheng, Z.; Liu, M.; Ganapathy, S.; Li, C.; Li, Z.; Zhang, X.; He, P.; Zhou, H.; Wagemaker, M. J. J. Revealing the Impact of

Space-Charge Layers on the Li-Ion Transport in All-Solid-State Batteries. *Joule* 2020, 4, 1311–1323.³ The Li-ion transport over the space-charge layer is quantitatively revealed by 2D NMR exchange experiments, demonstrating that the activation energy for Li-ion exchange increases significantly because of the presence of the space-charge layer, lowering the exchange current density and raising the internal resistance.

Ganapathy, S.; Yu, C.; van Eck, E. R. H.; Wagemaker, M. Peeking across Grain Boundaries in a Solid-State Ionic Conductor. *ACS Energy Lett.* 2019, 4, 1092–1097.⁴ Exploiting

Received: October 1, 2021

Published: January 13, 2022



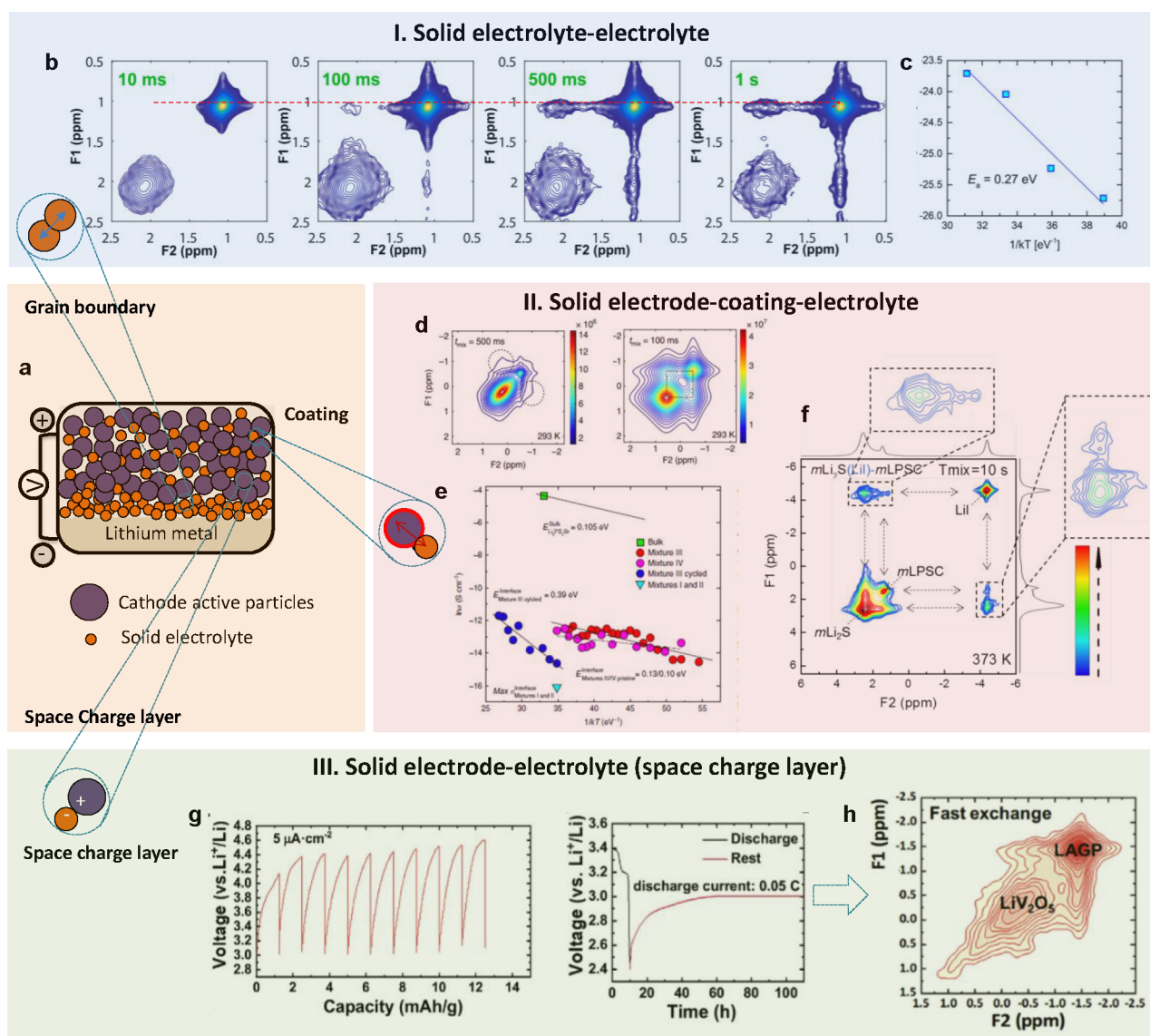


Figure 1. (a) Schematic figure showing how various interface aspects affect the Li-ion transport over the interfaces in an inorganic SSB. (b) 2D ${}^6\text{Li}$ – ${}^6\text{Li}$ exchange spectra of the mixture of $\text{Li}_6\text{PS}_5\text{Br}$ and $\text{Li}_6\text{PS}_5\text{Cl}$ nanopowders measured at 25 °C. (c) Temperature dependence of the diffusion coefficient obtained from fitting the increase in cross peak intensity as a function of mixing time to a diffusion model. Reproduced with permission from ref 4. Copyright 2019 American Chemical Society. (d) NMR measuring the spontaneous lithium-ion transport between the $\text{Li}_6\text{PS}_5\text{Br}$ SE and the Li_2S cathode before and after cycling. (e) Comparison of the Li-ion bulk and interface conductivities. Bulk Li-ion conductivity of $\text{Li}_6\text{PS}_5\text{Br}$ is determined by ${}^7\text{Li}$ ssNMR spin–lattice relaxation (SLR) experiments and the conductivity over the $\text{Li}_6\text{PS}_5\text{Br}$ – Li_2S interface from 2D/1D NMR exchange experiments for different cathode mixtures. Reproduced with permission from ref 24. Copyright 2017 The Authors. Published by Springer Nature under a Creative Commons Attribution 4.0 International License. (f) 2D ${}^6\text{Li}$ – ${}^6\text{Li}$ exchange spectra of the mixture of $\text{Li}_6\text{PS}_5\text{Cl}$ and Li_2S –Li powders measured at a spinning speed of 10 kHz at 100 °C and a mixing time of 10 s. Reproduced with permission from ref 28. Copyright 2021 The Authors. Published by Springer Nature under a Creative Commons Attribution 4.0 International License. (g) Determination of equilibrium potential of $\text{Li}_{1+x}\text{Al}_x\text{Ge}_{2-x}(\text{PO}_4)_3$ (LAGP) and $\text{Li}_x\text{V}_2\text{O}_5$ by GITT and galvanostatic discharging. (h) Representative solid-state 2D NMR ${}^6\text{Li}$ exchange spectra for LiV_2O_5 -LAGP. Reproduced with permission from ref 3. Copyright 2020 Elsevier.

the grain boundary with two-dimensional ${}^6\text{Li}$ – ${}^6\text{Li}$ exchange NMR on a mixture of $\text{Li}_6\text{PS}_5\text{Br}$ and $\text{Li}_6\text{PS}_5\text{Cl}$, Li exchange between particles of these two materials across grain boundaries was observed, allowing direct and unambiguous quantification of this often limiting process in solid-state electrolytes.

1. DIRECT MEASUREMENT OF LI-ION KINETICS AND LITHIUM DISTRIBUTIONS IN SES

Environmental issues have arisen from the continuous use of conventional energy resources, which are limited in supply.⁵

Tackling this requires a tremendous effort in finding suitable energy conversion and storage systems. Among them, Li-ion batteries have rapidly dominated the market due to their advantageous volumetric/gravimetric energy density and long cycle life.⁶ However, the use of liquid organic electrolytes in Li-ion batteries raises safety issues, in particular for relatively large systems as employed in electrical cars and grid storage.⁷ The safety issues of Li-ion batteries with liquid electrolytes have motivated the development of solid-state electrolytes, already since the early days of Li-ion batteries.^{8,9}

Intensive research efforts have led to several families of excellent inorganic solid Li-ion conductors, solid electrolytes (SEs), including the sulfides ($\text{Li}_2\text{S}-\text{P}_2\text{S}_5$, $\text{Li}_2\text{S}-\text{SiS}_2$, $\text{Li}_2\text{S}-\text{GeS}_2$), oxides ($\text{Li}_7\text{La}_3\text{Zr}_2\text{O}_{12}$ and $\text{Li}_{3x}\text{La}_{2/3-3x}\text{TiO}_3$) and phosphates (LiPON , $\text{Li}_{1+x}\text{Al}_x\text{Ge}_{2-x}(\text{PO}_4)_3$, $\text{Li}_{1+x}\text{Ti}_{2-x}\text{Al}_x(\text{PO}_4)_3$).^{10,11} The organic solid electrolytes (SEs) mainly refer to polymer electrolytes, where polyether based structures are the most well-known and extensively studied family. This is because poly ethylene oxide (PEO)-based polymers can directly complex with lithium salts and function as polymer electrolytes, without the addition of a liquid plasticizer.¹² However, to date, neither of these individual SEs fulfill the challenging combination of high conductivity, electrochemical stability, flexibility, and ease of processing, prerequisites for high-performance long cycle life solid-state batteries (SSBs). This has initiated the investigation of hybrid SE (HSE) concepts, where HSEs are usually a combination of inorganic and organic SE materials.^{13,14}

Typical inorganic SSBs introduce interfaces (grain boundaries) between SE particles as well as between SE and electrode particles. For specific combinations of SE and electrode, the latter have been shown to form the bottleneck in Li-ion transport, due to contact lost (strain induced due to electrode volume changes) and decomposition reactions (resulting in a higher resistance and/or strain due the formation of decomposition products) at the interfaces.^{13,15} The difficulty in selective detection and monitoring of Li-ion mobility makes quantification of the diffusional barriers posed by interfaces, understanding the role of interface properties and processes on the Li-ion transport a challenging task. A related challenge is detecting the quantitative distribution of Li in Li-metal anodes in contact with SEs, especially during battery operation. This has motivated the use and development of several microscopic and spectroscopic characterization approaches, mostly under ex-situ or in situ conditions as operando characterization is even more challenging.¹⁶ Initially, solid-state electrolytes were suggested to open the door to safe application of Li metal by suppressing dendrite formation.¹⁷ However, direct evidence has shown that lithium dendrites/filaments tend to grow along the grain boundaries and also through crystallites of the inorganic SEs, thus posing a hurdle to safe commercialization of Li-metal SSBs.^{18–21}

In this Account, recent investigations on fundamental studies of Li-ion transport and Li plating for SEs using solid-state Nuclear Magnetic Resonance (ssNMR) and Neutron Depth Profiling (NDP) will be reviewed. Through the ability of solid-state NMR to selectively probe Li, we demonstrate how it can be used to reveal and quantify the Li-ion diffusion through solid-state batteries. Next we demonstrate the use of operando Neutron Depth Profiling (NDP) providing a nondestructive view on Li migration, and Li density distribution as a function of depth under realistic (dis)charge conditions. By providing a direct view on Li, we underline the important role that both ssNMR and NDP can play in understanding critical processes, supporting the development of SSBs and their materials.

2. LI DIFFUSION OVER INTERFACES AND INTERFACE STRUCTURE PROBED BY SOLID-STATE NMR

NMR measurements are based on the interactions of the nuclear magnetic moment with an electromagnetic field in the radio frequency (RF) range while a strong magnetic field \mathbf{B}_0 is applied.²² The NMR signal shift and line shape are determined by the internal interactions, e.g., chemical shifts, Knight shifts,

and Fermi contact shifts, as well as dipolar and quadrupolar interactions.²² Recently ssNMR was demonstrated to enable selective measurement of the equilibrium Li-ion exchange current density over SE–electrode interfaces,^{23,24} providing added value to conventional electrochemical impedance spectroscopy used to measure conductivities.^{1,3,4,25} ssNMR has proven powerful in resolving subnano domains of the interfacial environments¹ and in addition allows us to monitor the Li-ion transport pathways through SEs by isotope replacement, thus making it possible to disentangle the complex Li-ion transport pathways in HSEs.^{1,26} To demonstrate this, we discuss the use of ssNMR in probing the Li-ion transport over different types of interfaces in the following sections. The solid-state NMR measurements reported in this work were mainly performed on a Bruker Ascend 500 magnet ($\mathbf{B}_0 = 11.7 \text{ T}$) with a NEO console located at the Radiation Institute Delft of the Delft University of Technology, and part of the research infrastructure of the battery research group in Delft.

2.1. Inorganic–Inorganic Interfaces, the Impact of Grain Boundaries on Li-Ion Transport

The high conductivity of several recently developed inorganic SEs, fulfills one of the prerequisites for SSBs. Much less established, however, is the role of grain boundaries between SE particles and between SE and electrode particles, the impact of interfacial coatings and that of space charges, and how these affect the conductivity. Making use of the ability of ^6Li NMR to distinguish between various Li-ion environments in the different phases, the equilibrium diffusion of Li ions over various grain boundaries in cathodic solid-state battery mixtures was quantified. In this way, it is possible to establish how the nature of the interface impacts the Li-ion kinetics, and what role this plays in the performance of SSBs, as illustrated by the following studies (Figure 1a).

Solid Electrolyte–Solid Electrolyte Interface. To measure the Li-ion diffusion over the grain boundaries within SEs with NMR, between different SE particles separated by a grain boundary, is intrinsically challenging as it does not provide contrast in chemical shift of the Li species. For this reason, $\text{Li}_6\text{PS}_5\text{Cl}$ and $\text{Li}_6\text{PS}_5\text{Br}$ were thoroughly mixed, exploiting the difference in ^6Li chemical shift of the Cl- and Br-containing variants of the argyrodite (due to the difference in Li-ion shielding by the difference in electronegativity of the halogens), as observed in Figure 1b, where both resonance signals are clearly distinguishable.⁴ The exchange spectroscopy (EXSY) experiment is a homonuclear spectroscopy experiment under equilibrium conditions where magnetization transfer from one site to another site can be observed. Because the Li ions carry the magnetization, this allows us to quantify the spontaneous diffusion between chemically inequivalent sites. Note that magnetization transfer could also occur through spin diffusion; however, these will not be transmitted through grain boundaries and would practically be independent of temperature, unlike the results presented here. Because the experiment is under equilibrium conditions, the measured Li-ion exchange represents the exchange current density over the interface. An EXSY experiment measures the ^6Li spectrum at $t = 0 \text{ s}$, then waits a “mixing time” T_{mix} and subsequently measures the ^6Li spectrum again at $t = T_{\text{mix}}$ (Figure 1b). The off-diagonal resonances appearing, quantify the amount of Li ions that spontaneously moved between these observed Li environments during t_{mix} .²⁴ It is important to note there is no

net transport of Li ions, as the measurements are performed under equilibrium conditions, and thus the exchange can be used to determine the self-diffusion, from which the conductivity can be determined. Exchange between the $\text{Li}_6\text{PS}_5\text{Br}$ and $\text{Li}_6\text{PS}_5\text{Cl}$ phases was quantified by fitting the evolution of the cross-peak intensity as a function of T_{mix} to a diffusion model derived from Fick's law as shown in Figure 1c, yielding an effective activation energy of 0.27 eV over the interface/grain boundary. This is comparable to the activation energy obtained for bulk diffusion measured by NMR relaxometry for the $\text{Li}_6\text{PS}_5\text{Cl}$ argyrodite,²³ demonstrating that the grain boundaries do not present a rate-limiting step for long-range Li-ion diffusion. This can be related to the large ductility of argyrodite and can also be expected to depend on the preparation of the pressed pallet.

Solid Electrolyte–Electrode Interface. From the previous paragraph it was concluded that the grain boundaries between ductile argyrodite particles does not form an additional bottleneck for Li-ion transport. However, the SE–electrode interface poses very different challenges, such as the possible presence and formation of decomposition reactions as well as contact loss upon cycling, impeding Li-ion transport over the interface. Making use of the different ^7Li chemical shift in the $\text{Li}_6\text{PS}_5\text{Br}$ argyrodite SE and the Li_2S cathode, 2D exchange experiments were able to quantify the diffusivity over the interface under different cathode preparation conditions, a snapshot of which is shown in Figure 1d.^{23,24} As can be seen in Figure 1e, the effective conductivity over the SE–electrode interface in a pristine cathodic mixture is orders of magnitude lower than the bulk conductivity of SE. Nano sizing the SE through mechanical milling, as well as mechanical mixing of the $\text{Li}_6\text{PS}_5\text{Br}$ argyrodite and the Li_2S cathode, is required to achieve a sufficient ion contact area, and thus a sufficiently large equilibrium flux, and from that the estimated conductivity, over the interface to even measure the Li-ion exchange. However, upon cycling, the 2D exchange experiments show that the interface conductivity is drastically lowered, which can be associated with contact loss and formation of poorly conducting decomposition products, such that it would dominate the overall resistance of the solid-state battery (Figure 1d). In addition, the activation energy for Li-ion transport increases, most likely the result of the poorly conducting decomposition products (Figure 1e). An additional consequence of the narrow electrochemical stability window of the $\text{Li}_6\text{PS}_5\text{Br}$ argyrodite is that the redox activity of the argyrodite and its decomposition products, that is, the P^{5+}/P redox at the negative electrode and the S^{2-}/S redox at the positive electrode, will lead to additional capacity during battery cycling.²⁷ This exposes the interface challenges arising in electrode composites for SSBs and brings forward the need of interface designs to prevent the large increase in impedance during cycling, where volumetric changes (both induced by electrode volumetric changes upon (de)lithiation and due to SE decomposition arising from redox instabilities) appear responsible.

Impact Interface Coating on the Solid Electrolyte–Electrode Interface. As discussed above, a key challenge for SSBs is to design electrode–electrolyte interfaces that combine (electro)chemical and mechanical stability while allowing facile Li-ion transport. Typically, this presents conflicting demands. The SE–electrode interface area, ionic contact area, should be maximized to facilitate high currents, while it should be minimized to reduce the parasitic interface reactions and

enhance stability. Addressing these issues would benefit from establishing the impact of interface coatings on local Li-ion transport over grain boundaries. As shown in our recent work,²⁸ Li-ion transport between three phases, i.e., between SE ($\text{Li}_6\text{PS}_5\text{Cl}$), electrode coating (LiI), and the electrode (Li_2S) in the cathodic mixture, can be measured using exchange NMR (Figure 1f). This allows us to disentangle the quantitative impact of an interface coating on the Li-ion transport in the cathodic mixture of the SSB. In this case, the $\text{Li}_6\text{PS}_5\text{Cl}$ (average particle size 50 μm) was not ball milled, as typically required to achieve sufficient ion contact area, and also the LiI– Li_2S particles are relatively large (average particle size 5 μm). The high diffusivity and very low activation energies for Li-ion transfer from Li_2S to LiI and from $\text{Li}_6\text{PS}_5\text{Cl}$ to LiI, 0.142 and 0.117 eV, respectively, are similar to that for overall Li-ion transfer between Li_2S and $\text{Li}_6\text{PS}_5\text{Cl}$ in the presence of the LiI coating. This indicates that LiI facilitates the Li-ion transport and thus functions as a bridge between electrode and electrolyte. These NMR experiments demonstrate that the presence of the LiI coating in this case enhances the interface transport to such an extent that the commonly applied strategy of nanosizing of the cathodic mixture can be abandoned. SSBs using this coating demonstrate facile sulfur activation, while at the same time minimizing SE decomposition by use of micron-sized particles in the cathodic mixtures, enabled by facilitating easy Li-ion transport over the SE–cathode interface.

The Role of Space Charges at Solid Electrolyte–Electrode Interfaces. It has been proposed that space-charge layers at the electrode–SE interfaces can hinder diffusion, thus raising the internal resistance in SSBs.²⁹ However, the influence of space-charge layers on the ionic charge transport in SSBs is challenging because of the difficulty to distinguish it from other contributions to the overall diffusion over the interface. To address this, the impact of the space-charge layer was measured between a $\text{Li}_x\text{V}_2\text{O}_5$ electrode and a $\text{Li}_{1+x}\text{Al}_x\text{Ge}_{2-x}(\text{PO}_4)_3$ (LAGP) SE. This was achieved by changing the potential of the $\text{Li}_x\text{V}_2\text{O}_5$, through its composition, and selectively measuring the ion transport over the $\text{Li}_x\text{V}_2\text{O}_5$ –LAGP interface, again by 2D exchange NMR.³

A space-charge layer is formed due to the difference in chemical potential of Li between the electrode and the SE. For instance, if the Li chemical potential is lower in the positive electrode, Li ions will be driven from the SE to the positive electrode (assuming that the SE is unable to accommodate the electron). The charge separation stops when the potential difference compensates the difference in Li chemical potential. Tuning the chemical potential of the $\text{Li}_x\text{V}_2\text{O}_5$ positive electrode was accomplished through its composition. As can be observed in Figure 1g, a large spontaneous Li-ion exchange current density was observed using ^6Li EXSY 2D exchange NMR between the LiV_2O_5 electrode and LAGP SE under the condition that the space-charge layer is “switched off” (Figure 1h), which is achieved by matching the Li chemical potential of LiV_2O_5 and LAGP. When the space-charge layer is “turned on”, by increasing the Li chemical potential (lowering its intercalation voltage) in $\text{Li}_x\text{V}_2\text{O}_5$, the Li-ion exchange is reduced and the activation barrier increases. Under the assumption that preparation of the two electrode mixtures leads to comparable interfaces, this indicates that the charge distribution due to the space-charge layer at the interface between electrodes and SEs can contribute significantly to the interface resistance in SSBs.³

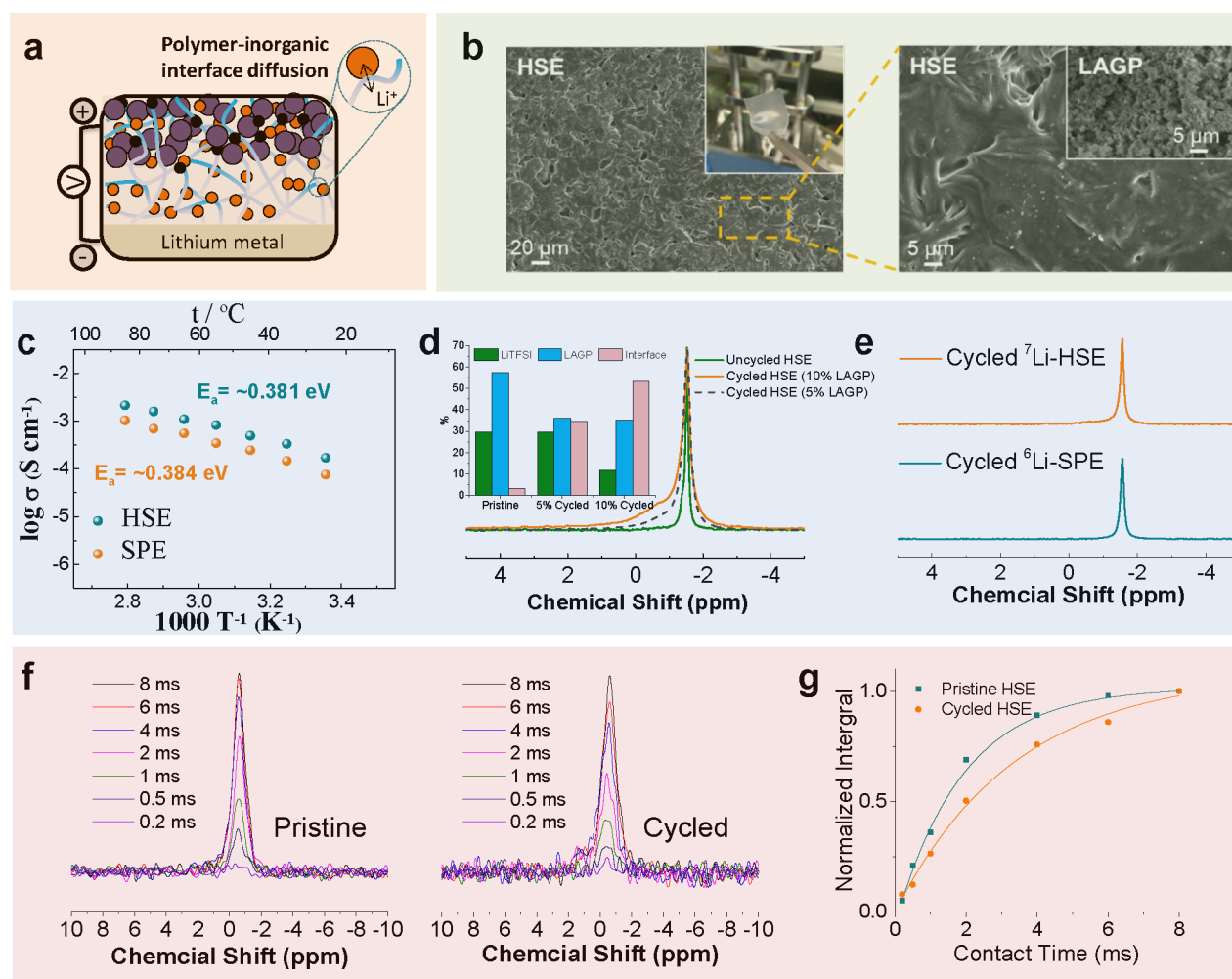


Figure 2. (a) Schematic figure illustrating the interfacial barrier between the organic–inorganic components in a SSB with a HSE. (b) SEM measurements showing the morphology of the HSE and the LAGP particles. (c) Ionic conductivity determined by impedance spectroscopy measurements of the HSE and solid polymer electrolyte (SPE) at different temperatures. (d) 1D ^6Li MAS spectra of the HSE and HSE cycled between ^6Li metal and their quantification of the different species. (e) 1D ^6Li MAS spectra of the SPE cycled between ^6Li metal and HSE cycled between ^7Li metal. (f,g) ^1H – ^6Li CP spectra as a function of contact times for (f) pristine HSE electrolyte and cycled HSE between $^6\text{LiFeO}_4$ and $\text{Li}_4\text{Ti}_5\text{O}_{12}$, and (g) CP build-up plots. Reproduced with permission from ref 1. Copyright 2019 American Chemical Society.

These results present an overview of how various interface aspects can affect the Li-ion transport, summarized in Figure 1a, demonstrating that interfaces represent one of the main challenges for SSBs. In the case of argyrodite SE, while grain boundaries are not rate limiting, the interfaces between the SE and Li_2S cathode particles are. To overcome this, the interface area between the argyrodite SE and Li_2S cathode is required to be sufficiently large, highlighting the importance of particle size and intensive mixing of the cathode and SE. During battery cycling, however, the initially beneficial large interface area turns into a pitfall when cycled outside the electrochemical stability window of the SE. Volumetric changes occur and decomposition products are formed, turning the interface into a barrier for Li-ion diffusion. To mitigate this, we have demonstrated how a suitable interface material or coating can lower the grain boundary resistance, which allows reducing of the ionic contact area between SE and electrode particles (and thus larger SE and cathode particles), reduces the overpotentials, and thus diminishes decomposition reactions. But when a stable and Li-ion conducting interface can be achieved, differences in chemical potentials between SE and electrodes can result in space-charge layers that can form an additional

barrier to Li-ion transport. Summarizing, these results signify that the “interface problem” is multifaceted and that interface research and design strategies are paramount for the development of long functioning SSBs.

2.2. Inorganic–Organic Interfaces in Hybrid SEs, the Role of Phase Boundaries

An alternative for inorganic SEs are hybrid solid electrolyte (HSE) concepts,²⁶ which combine an organic polymer electrolyte with an inorganic SE, where the polymer phase has the potential to enhance the electrolyte–electrode interface contact and can provide intrinsic flexibility to maintain this during cycling, offering practical application potential.^{30–32} To date, polymer electrolytes exhibit a relatively low Li-ion conductivity; however, inorganic fillers can be used in two distinct ways to increase the ionic conductivity, as has been examined by ssNMR.^{31,32} First, the ionic conductivity of the polymer electrolyte can be enhanced by introducing a nanosized inorganic filler, which effectively lowers the glass-transition temperature through the large inorganic–organic interface area, thereby increasing the PEO chain mobility.^{33,34} Second, when micron-sized conductive inorganic SE particles

are introduced as inorganic filler, the polymer SE dominantly acts as a flexible host. The latter is effective, especially for large amounts of inorganic solid filler, usually beyond 50 wt %, ^{33,34} but has the potential drawback that the organic–inorganic interfaces lead to a high barrier for Li-ion transport as indicated in Figure 2a.

The most intensively investigated HSEs are based on PEO, incorporating different ion conducting fillers. Structural analysis using synchrotron nanotomography revealed for a PEO-Li₇La₃Zr₂O₁₂ (LLZO) HSE that the inorganic LLZO particles are highly aggregated in the polymer electrolyte matrix.³⁵ In combination with atomic force microscopy, this elucidated the origin of the heterogeneous interfacial properties, where the PEO molecular weight was shown to dictate the electrochemical performance.¹³ In addition to the microstructure, it is important to determine the Li-ion transport pathway through such heterogeneous electrolytes, to rationalize the overall conductivity and provide guidance for the design of optimal HSEs. Through high-resolution ssNMR in combination with selective isotope labeling, Hu et al.²⁶ were able to track the Li-ion pathways within a PEO-LLZO HSE by monitoring the replacement of ⁷Li in the composite electrolyte by ⁶Li from the ⁶Li-metal electrodes during battery cycling. They found in the case of an HSE with high weight fraction of the inorganic filler (50%) that the lowest path of resistance for Li-ion transport is through the LLZO ceramic phase, instead of through the PEO-LLZO interface regions or through the PEO bulk.²⁶ The ion transport pathways shift from the LLZO ceramic component to the PEO polymer phase when the LLZO content is decreased from 50 to 5 wt %.³⁴ Even the best conductivity achieved, $\sim 10^{-5}$ S/cm, is insufficient for room temperature operation of the HSE in a SSB. The conductivity of the PEO is insufficient at low LLZO content, and at high LLZO content LLZO agglomeration blocks the ion transport pathways through the PEO phase, whereas diffusion from one LLZO particle to another is impeded by its large activation energy.³⁶

Recently, we developed an HSE that makes optimal use of the high conductivity of the inorganic SE and the flexibility of the polymer matrix.¹ As observed in Figure 2b,c, an HSE composed of PEO-succinonitrile(SN)-LiTFSI and LAGP was prepared, resulting in a room temperature conductivity of 1.73×10^{-4} S/cm at 25 °C. To reveal the role of the LAGP phase in the Li-ion transport of the HSEs, ssNMR was employed. The HSE was cycled between two ⁶Li-metal sheets, and thus the ⁷Li in the solid electrolyte that takes part in the Li-ion transport will be partially replaced by ⁶Li. Subsequently, ⁶Li NMR is used to locate ⁶Li in the solid electrolyte and reveal the diffusion pathway. As can be observed in Figure 2d,e, after cycling the HSE between ⁶Li metal, a clear increase in the ⁶Li signal in both the LAGP and the interface environment (located at -0.75 ppm) was observed. This shows that Li-ion transport is mediated by both the organic and inorganic phase and that the interface between the phases does not pose a significant barrier. This tandem Li-ion transport, through both organic and inorganic phases, allows activation of micron-sized inorganic particles, where even low filler amounts (10 wt %) can achieve conductivities that allow room temperature operation, offering a promising route for HSEs.¹

The key toward activating high conductivity of the inorganic SE component lies in the nature of the interface between the inorganic and organic phases,²⁶ of which relatively little is known. To further resolve the interface structure, 1D ¹H–⁶Li

cross-polarization (CP) ssNMR experiments were carried out. In this experiment, transfer of polarization occurs from the protons (¹H), in this case present in the polymer phase, to any ⁶Li environment in its close vicinity (within a few atomic bond lengths). For both the pristine HSE, and that cycled between ⁶Li enriched LiFePO₄ and Li₄Ti₅O₁₂, the ¹H–⁶Li CP MAS NMR spectra reveal one Li environment at -0.75 ppm, which increases in intensity as the contact time increases (Figure 2f).¹ This indicates that the observed ⁶Li environment is in close spatial proximity (within a few atomic bond lengths) to the polymer phase of the HSE. In addition, as it only appears in the presence of the LAGP phase, we conclude that it must represent the interface environment between the LAGP and the polymer phase in the HSE. Therefore, ⁶Li CP MAS NMR analysis enables nondestructive access to the interface environment between the polymer and inorganic fillers, which is difficult, if not impossible, by any other traditional characterization method.¹ The observation that the CP intensity buildup is weaker for the cycled HSE (Figure 2g) may indicate that locally the ⁶Li ions are more mobile after cycling, which weakens the ¹H–⁶Li dipolar interaction, making the CP less efficient. The ability to selectively access Li ions at the interfaces is yet another example of the versatility of ssNMR which especially comes into play for HSEs.

In future experiments, we aim for further characterization of interface environments with respect to Li-ion transport, considering a comprehensive evaluation of salt concentration and interface modifications. Overall, the presented results illustrate the use of ssNMR in monitoring the transport of Li ions across interfaces through isotope enrichment and 2D exchange experiments, and identifying the interface environments through CP experiments, which we expect to play an important role in revealing structure–performance relationships in future HSE studies. Because most elements (nonzero spin nuclei) can be selectively probed by solid-state NMR, the presented approaches can be expected to be more generally applicable, for instance for other battery chemistries such as Na⁺, Mg²⁺, and Al³⁺ batteries.

3. LI PLATING/STRIPPING IN SE LI-METAL BATTERIES PROBED BY OPERANDO NDP

The difficulty in developing large capacity positive electrodes has led to a renewed interest in Li-metal anodes. It combines the ultimate capacity (3860 mAh/g compared to 370 mAh/g for standard graphite anodes) with the lowest redox potential (-3.04 V versus standard hydrogen), making Li metal the ideal anode with respect to the battery energy density.^{37–39} Especially, the combination with SEs is believed to open the door to safe application of Li metal under the assumption that dendrite formation can be suppressed.¹⁷

However, direct evidence from in situ X-ray tomography has shown that lithium dendrites/filaments tend to grow along grain boundaries of inorganic solid-state electrolytes,^{18,19,40} or even through SE crystallites,²⁰ demonstrating that inhomogeneous lithium metal deposition causes short-circuiting even in SSBs.^{40,41} The same challenges appear present in HSEs in combination with Li-metal anodes, as short circuits and an increase in overpotential are observed in symmetrical Li-metal cells with HSEs,^{2,42} reflecting both dendrite growth and delamination.

SE research would benefit from the development of quantitative and noninvasive operando techniques that detect

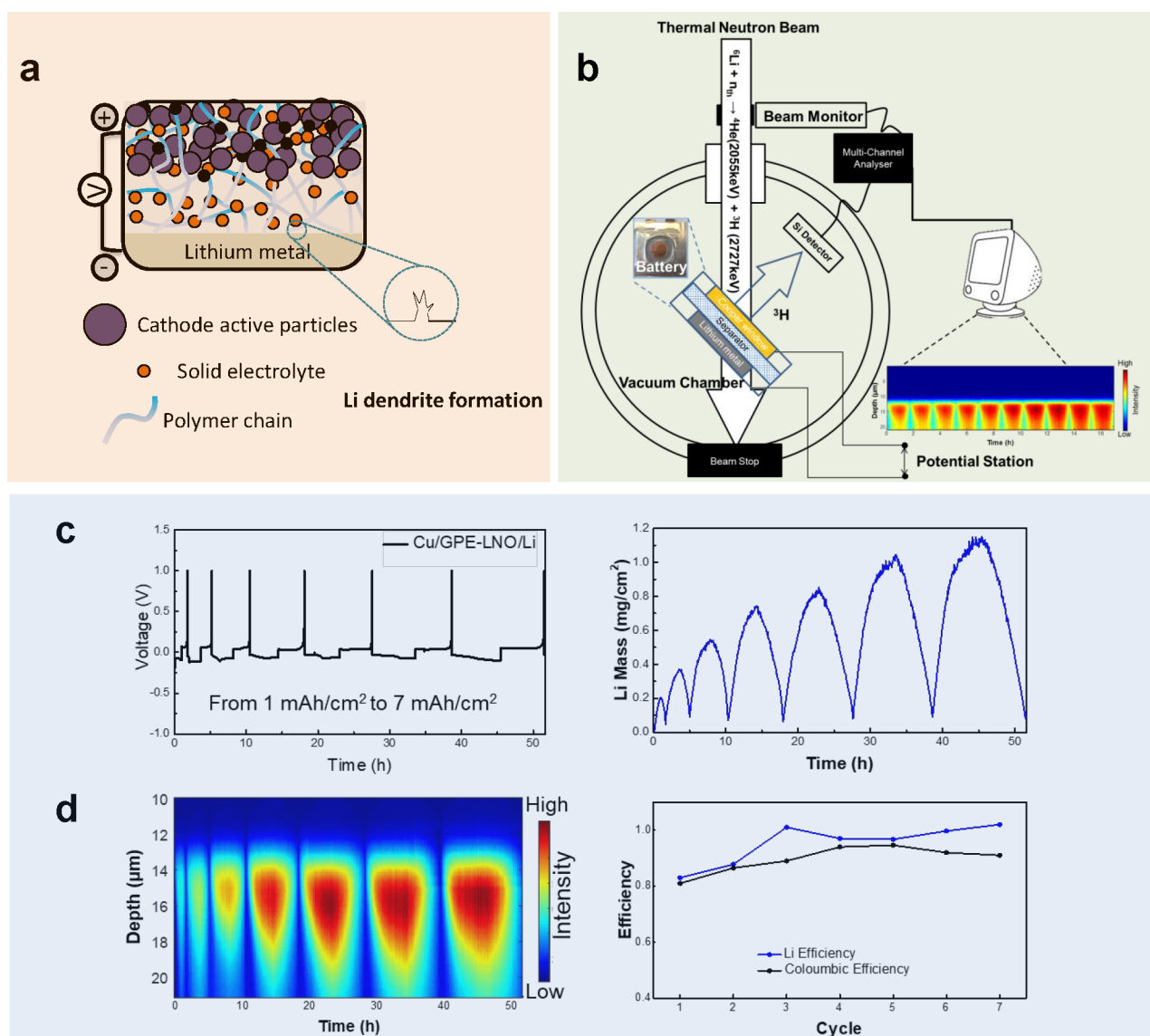


Figure 3. (a) Schematic figure illustrating Li dendrite formation in a SSB with a HSE. (b) Principle of operando NDP for Li-metal plating and stripping. (c,d) Electrochemical performance, Li distribution, Li mass, and Li efficiency from operando NDP of the Cu/Gel polymer electrolyte with LiNO_3 additive/Li battery at 1 mA/cm^2 for 1 to 7 h. Reproduced with permission from ref 52. Copyright 2019 American Chemical Society.

Li, while operating under realistic battery conditions. Recently, operando ^7Li ssNMR has been shown to be very promising in this context. It can distinguish differences in the Li-metal microstructure based on differences in the bulk magnetic susceptibility and is able to quantify the amount of “dead” Li metal and Li in the SEI during cycling.^{43–45} Another technique directly probing Li is operando NDP, where enabling the use of pouch cells opened the door to the study of the Li-metal density as a function of electrode depth under realistic battery operation.⁴⁶ Neutron-based characterization techniques have unique advantages as it enables us to probe the bulk material homogeneously (because of the low attenuation in most materials), low-energy deposition in the material of interest and due to the complementary scattering cross sections as compared to X-ray and electron sources, which for instance enables the observation of light atoms (e.g., H, Li, O). NDP is isotope specific, where only a few elements offer a sufficiently large enough cross section for the capture reaction of a thermal or cold neutron (e.g., ^{10}B and ^6Li). It can be considered a

noninvasive and nondestructive technique due to the low amount of capture reactions in the thermal or cold neutron beam. With respect to Li metal, this technique allows operando monitoring of the formation of inactive Li (in the SEI and as “dead” Li metal, which cannot be distinguished) and the Li density evolution upon plating-stripping.² NDP introduced in this work was performed at the thermal neutron beamline A of the 2MW pool-type research reactor at the Reactor Institute Delft (RID) of the Delft University of Technology, a facility that is directly accessible for the battery research group in Delft.

3.1. Dendrite Penetration

Recently, as observed by X-ray tomography, it appears that the mechanism of dendrite growth is very different in solid electrolytes than in liquid electrolytes,^{46–48} where one important factor appears to be the applied pressure that typically exceeds the yield strength of Li metal ($\sim 0.8 \text{ MPa}$). Dendrite growth is believed to induce preferential deposition on local inhomogeneities like grain boundaries and voids

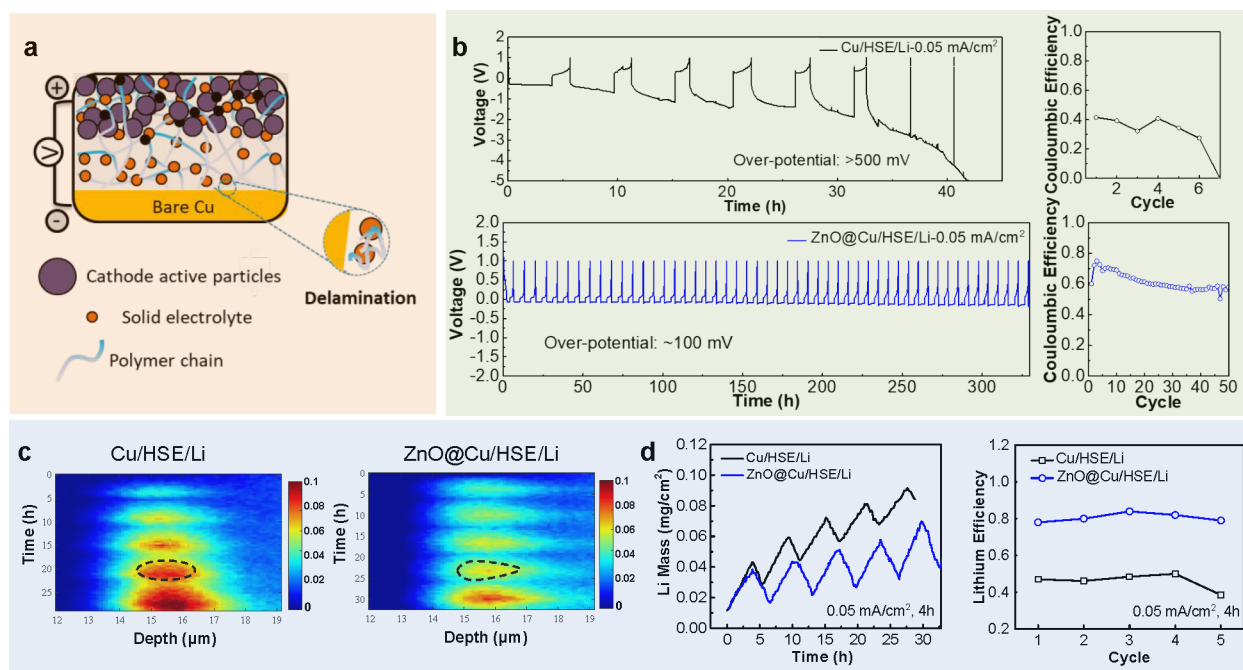


Figure 4. (a) Schematic figure showing the delamination in a SSB with a HSE and bare Cu. (b) Electrochemical performance of the Cu/HSE/Li and ZnO@Cu/HSE/Li battery at 0.05 mA/cm² for 4 h. (c,d) Li distribution, Li mass, and Li efficiency from operando NDP measurements for five cycles of the Cu/HSE/Li and ZnO@Cu/HSE/Li batteries at 0.05 mA/cm². Reproduced with permission from ref 2. Copyright 2020 American Chemical Society.

present at the Li-metal electrolyte interfaces, resulting in local hotspots of high current. The larger molar volume of Li metal, when compared to Li in SEs,^{47,49} has been suggested to cause local expansion, causing cracks filled with Li-metal deposits.⁴⁴ The quick polarization before a short circuit typically occurs in SSBs due to dendrite induced decomposition (leading to poorly conducting species that raise the resistance), which underlines the interlinked problem of dendrite formation and the instability of most SEs toward the low reduction potential of Li metal (Figure 3a). Indeed most SEs are predicted to be unstable toward Li metal,⁵⁰ which is especially exacerbated through the high surface area of dendrite filaments in SSBs.

Operando ⁷Li ssNMR is a direct probe of Li under realistic cell conditions and has been demonstrated to distinguish differences in the Li-metal microstructure quantitatively.^{43–45} NMR relies on the radio frequency field to excite the Li nuclei, which has a limited penetration in metals. This so-called skin depth is given by the relationship: $d = (1/\sqrt{\pi\mu_0})\sqrt{\rho/\mu_r f}$, where μ_0 is the permeability of vacuum, μ_r is the relative permeability of the metal, ρ is the density of the metal, and f is the applied radio frequency field.⁴⁵ For instance for a 500 MHz (11.4 T) applied magnetic field and the ⁷Li radio frequency field, the skin depth is 11 μ m in Li metal. If the Li-metal features are much smaller than this, this implies that most of the Li metal will be observed by NMR and that quantitative analysis can be realized.⁴⁵ In previous in situ/operando ssNMR studies on Li-metal plating/stripping, the counter anode is a Li-metal strip,^{44,51} which gives rise to resonance at ~245 ppm when placed perpendicular to the fixed magnetic field B_0 and ~270 ppm when the strip is parallel to B_0 , a consequence of the bulk magnetic susceptibility.⁵¹ As a consequence, differences in Li-metal microstructures can be distinguished with ssNMR, so far only exploited for liquid electrolytes. The pressure required for typical SSB configurations is challenging,

in the context of which HSEs may actually be less challenging as these typically require a lower pressure.

Similarly, it is challenging to apply pressure in batteries for operando NDP measurements. NDP has been used to study the Li-ion transport in Li-metal gel polymer batteries, providing a direct view on the Li-metal plating and stripping.⁵² The schematic experimental setup of NDP is shown in Figure 3b. NDP utilizes the exothermal neutron capture reaction with ⁶Li resulting in the following reaction: ${}^6\text{Li} + n_{\text{thermal}} \rightarrow {}^4\text{He}^{2+} (2.06 \text{ MeV}) + {}^3\text{H}^+ (2.73 \text{ MeV})$. When this takes place within a battery, the charged particles produced (⁴He²⁺ and ³H⁺) that have a well-defined starting energy, will lose part of their kinetic energy due to transmission through the electrode and the current collector/window toward the detector, which is quantified by the stopping power.⁵² The stopping power is directly related to the composition and density of the materials, in many cases a known quantity (which can change during battery cycling making data analysis more complex). Therefore, by measuring the energy loss of the ⁴He²⁺ and ³H⁺ ions, when they exit the electrode, the depth of the capture reaction can be determined.^{52,53} There are only a few stable atoms that have a sufficiently large capture cross section (including ¹⁰B and ⁶Li) to determine depth profiles. The maximum depth that can be probed, as well as the resolution, depends on the stopping power of the material of interest. Here the general trend is that a higher density results in a higher stopping power, leading to a smaller maximum depth that can be probed in combination with a better depth resolution.⁵³ In principle, there is no lateral limitation for the sample, where typically sample surfaces of a cm² are used which matches typical lab scale batteries.

As shown in Figure 3c, NDP allows direct measurement of Li-ion concentration profiles perpendicular to the electrode/electrolyte interface with a resolution of approximately 100 nm

up to a micrometer (depending on the measurement conditions) under realistic battery operation.⁵² This makes it possible to measure for instance Li-ion gradients that can reveal the origin of the restricted power density in batteries. Additionally, NDP can be used to monitor dendrite formation at Li-metal anodes through the electrolyte by the increasing Li-concentration within the electrolyte region. Both aspects provide crucial information for improved battery design.⁵² As an example, shown in Figure 3c,d, the lithium anode plating and stripping in the gel polymer electrolyte with LiNO₃ additive was monitored with operando NDP from 1 up to 7 mAh/cm². The evolution of Li density as well as the Li efficiency during cycling have been shown, illustrating the unique ability of NDP in monitoring electrochemical Li plating/stripping.⁵² It should be stressed that the Li efficiency, defined as the ratio of the stripped to the plated amount of Li within the maximum depth probed by the NDP, provides complementary information to the electron efficiency as quantified by the Coulombic efficiency. The difference between the Coulombic efficiency and Li efficiency quantifies the amount of irreversible reactions that do not involve Li-ion transfer, such as direct electrolyte reduction and chemical dissolution of Li from the SEI.⁵²

Recently, the application of NDP has been extended to SSBs utilizing inorganic electrolytes. Hu et al.⁵⁴ used NDP to study the interfacial behavior of a garnet type SE (LLZO) in contact with metallic Li through in situ monitoring of the Li plating/stripping processes. The NDP measurement demonstrates predictive capabilities for diagnosing short circuits in SSBs. Han et al.⁵⁵ investigated the origin of dendrite formation by monitoring the dynamic evolution of the Li concentration profiles in three important SEs (LiPON, LLZO, and amorphous Li₃PS₄) during lithium plating using operando NDP. Their findings demonstrate the ability of NDP in studying the different driving forces for dendrite formation in these SEs.⁵⁵

A challenging aspect of operando measurements of solid-state batteries is that the stopping power of the window facing the detector needs to be low and thus the window needs to be very thin, which complicates application of high and stable pressure, as typically required for SSB concepts. In this context, HSEs that often operate under lower pressures, within the limits of existing operando cells,^{56,57} are of initial interest for operando NDP studies. Recently, this allowed us to monitor the delamination of Cu/HSE/Li-metal cells, and the impact of the presence of a lithium-philic ZnO layer on the Cu to prevent this, as presented in the next paragraph.

3.2. Delamination

Investigating the Li-metal–SE interface under operando conditions is challenging, in the first place because the charged particles, which result from the capture reaction, need to pass the Li metal and the current collector window. As a consequence, a thick Li-metal film cannot be used, and an anode-less configuration is preferred, in which case the Li inventory is initially stored in the positive electrode (discharged state) (Figure 4a). In this case, the SE is directly facing the current collector, which also functions as a window sealing the battery from the surrounding environment. When the Li plating is examined during battery charging, the battery polarization is very high, Figure 4b. This is the result of delamination of the SE from the current collector upon repeated lithium–metal plating/stripping, resulting in early cell

death. To improve the HSE/Cu interface, we explored the introduction of a 100 nm thin ZnO film deposited via atomic layer deposition on the copper current collector, effectively making the current collector lithium-philic.² The “anode free” configuration using this ZnO@Cu electrode resulted in more reversible cycling, Figure 4b, offering a suitable SSB configuration for investigating operando Li-metal plating in a SSB.²

The results of the Li-metal plating in the solid-state Cu/HSE/Li and ZnO@Cu/HSE/Li batteries are provided in Figure 4c, yielding the normalized lithium–metal density (normalized to the bulk Li-metal density), as a function of depth, during five cycles at a current density of 0.05 mA/cm². For the bare copper current collector in the Cu/HSE/Li battery, the average Li density, as well as the thickness of the deposits, rapidly increase upon cycling, reflecting the buildup of inactive Li metal and Li species at the HSE side over cycling. This situation improves for the ZnO@Cu current collector, reflecting better affinity between Li metal and the ZnO-covered current collector, consistent with the improved electrochemical cycling shown in Figure 4c. Integrating the Li-density depth profiles, results in the evolution of the plated lithium mass during cycling. The ratio of the stripped capacity and the plated capacity represents the Li-efficiency, complementary to the Coulombic efficiency (electron efficiency). The presence of the ZnO film on the copper current collector increases the Li efficiency from ~45% to 80%, reflecting a more-efficient plating/stripping process as examined with NDP.²

These initial operando NDP studies of Li metal demonstrate the challenge of Li-metal anodes in SSBs as well as the complementary data provided by NDP as compared to available techniques. Lithium dendrites may grow along the phase boundaries of the organic and inorganic phases, causing a short circuit. In addition, especially for the “anode-less” or “anode-free” configuration it is very difficult to maintain the contact between Li metal and the HSE during cycling. Both the large volumetric changes of the Li-metal anode and SE decomposition can be held responsible for interface degradation and delamination. In future work, thin Li metal sputtered on the Cu current collector will enable more detailed operando NDP studies toward the Li-metal–SE interface, aiming at more fundamental understanding of the failure mechanisms.

4. CONCLUSIONS AND PERSPECTIVE

Understanding Li-ion transport and Li-metal plating in SSBs is challenged by the difficulty to quantify the Li distribution and its chemical form, in particular during realistic battery operation. Taking advantage of noninvasive and nondestructive state-of-the-art ssNMR and operando NDP techniques appears to have much potential to provide more insight in the behavior of Li and Li ions in SEs and SSBs. ssNMR has revealed and quantified ionic transport across grain boundaries and provided insight in the nature of the interface, and its role in the Li-ion transport. 2D exchange NMR allows monitoring the spontaneous equilibrium Li-ion diffusion between different Li environments, and cross-polarization experiments as one of several other NMR methods can access the interface structure. Moreover, isotope replacement can be used to track the Li ions in different SE phases and reveal the transport pathways. It is found that the bottleneck for charge transport in the studied SSBs is located at the interface between SE and electrode. Adjusting the interface properties is the key to solve this

problem, where many phenomena play a role, including composition, chemical bonding, wetting, and space-charge layers. Another challenge where ssNMR demonstrates large added value is the study of Li-metal anodes. To achieve inherent safe operation of Li-metal SSBs requires that Li-metal dendrite formation can be avoided or blocked. At low current densities and slow battery charging, SEs appear to satisfy these conditions; however, still our understanding of the onset and growth of dendrites is limited, due to the difficulties in studying these processes under realistic operation conditions. Anode-less or anode-free configurations set high demands on interface stability, which requires much more understanding of the role interfaces in electrochemical Li-metal plating and stripping. The ability of ssNMR to distinguish between different Li-metal morphologies and to quantify “dead” Li-metal under operando conditions is very promising, although development of operando cells is required to extend the application of this technique to higher pressures relevant for SSBs. Operando NDP also offers a multitude of possibilities for Li-metal anode research, enabling nondestructive monitoring of the Li-metal density as a function of electrode depth, providing insight into the onset of delamination and dendrite formation during cycling. With their ability to selectively probe Li, both techniques can be expected to play an important role in understanding processes in Li-based batteries, as explicitly demonstrated for Li-metal SSBs. This battery system itself poses significant challenges, where both techniques in combination with other advanced characterization techniques will provide guidance in material and interface design and development, aiming to achieve safe, high-energy-density energy storage system.

AUTHOR INFORMATION

Corresponding Authors

Ming Liu – Section Storage of Electrochemical Energy, Department of Radiation Science and Technology, Faculty of Applied Sciences, Delft University of Technology, Delft 2629 JB, The Netherlands; orcid.org/0000-0003-0569-7073; Email: liuming@sz.tsinghua.edu.cn

Marnix Wagemaker – Section Storage of Electrochemical Energy, Department of Radiation Science and Technology, Faculty of Applied Sciences, Delft University of Technology, Delft 2629 JB, The Netherlands; orcid.org/0000-0003-3851-1044; Email: M.wagemaker@tudelft.nl

Author

Swapna Ganapathy – Section Storage of Electrochemical Energy, Department of Radiation Science and Technology, Faculty of Applied Sciences, Delft University of Technology, Delft 2629 JB, The Netherlands

Complete contact information is available at: <https://pubs.acs.org/10.1021/acs.accounts.1c00618>

Notes

The authors declare no competing financial interest.

Biographies

Ming Liu received his Ph.D. from Tsinghua University and Hong Kong University of Science and Technology in 2017. After a postdoc (2017–2021) in the group of Prof. Marnix Wagemaker at the Delft University of Technology, he continued his career in Tsinghua

Shenzhen International Graduate School as an assistant professor for fundamental battery research.

Swapna Ganapathy graduated from the University of Pune with an M.Sc. in Chemistry and completed a Ph.D. in ssNMR from Leiden University in 2008. After a postdoc in the battery group of Prof. Marnix Wagemaker at the Delft University of Technology, she continued her career in his group as a permanent staff scientist exploring fundamental aspects of materials for both liquid and solid-state Li/Na-ion batteries.

Marnix Wagemaker received his Ph.D. in physics from the Delft University of Technology in 2003 and became a full professor in 2018. He received several grants, including a VICI and an ERC grant, for fundamental battery research and is leading the Storage of Electrochemical Energy group on battery research at the Delft University of Technology.

ACKNOWLEDGMENTS

The authors would like to thank Lihan Zhang at Tsinghua SIGS for his assistance with the TOC figure. Financial support is greatly acknowledged from The Netherlands Organization for Scientific Research (NWO) under the VICI grant no. 16122. Financial support from the Advanced Dutch Energy Materials (ADEM) program of the Dutch Ministry of Economic Affairs, Agriculture and Innovation is gratefully acknowledged.

REFERENCES

- (1) Liu, M.; Cheng, Z.; Ganapathy, S.; Wang, C.; Haverkate, L. A.; Tulodziecki, M.; Unnikrishnan, S.; Wagemaker, M. Tandem Interface and Bulk Li-Ion Transport in a Hybrid Solid Electrolytes with Microsized Active Filler. *ACS Energy Lett.* **2019**, *4*, 2336–2342.
- (2) Liu, M.; Wang, C.; Cheng, Z.; Ganapathy, S.; Haverkate, L. A.; Unnikrishnan, S.; Wagemaker, M. Controlling the Li-metal growth to enable low Li-metal excess all solid state Li-metal batteries. *ACS Mater. Lett.* **2020**, *2*, 665–670.
- (3) Cheng, Z.; Liu, M.; Ganapathy, S.; Li, C.; Li, Z.; Zhang, X.; He, P.; Zhou, H.; Wagemaker, M. J. J. Revealing the Impact of Space-Charge Layers on the Li-Ion Transport in All-Solid-State Batteries. *Joule* **2020**, *4*, 1311–1323.
- (4) Ganapathy, S.; Yu, C.; van Eck, E. R. H.; Wagemaker, M. Peeking across Grain Boundaries in a Solid-State Ionic Conductor. *ACS Energy Lett.* **2019**, *4*, 1092–1097.
- (5) Goodenough, J. B.; Park, K.-S. The Li-ion rechargeable battery: a perspective. *J. Am. Chem. Soc.* **2013**, *135*, 1167–1176.
- (6) Wagemaker, M.; Mulder, F. M. Properties and Promises of Nanosized Insertion Materials for Li-Ion Batteries. *Acc. Chem. Res.* **2013**, *46*, 1206–1215.
- (7) Dunn, B.; Kamath, H.; Tarascon, J.-M. Electrical energy storage for the grid: a battery of choices. *Science* **2011**, *334*, 928–935.
- (8) Kulkarni, A.; Maiti, H.; Paul, A. Fast ion conducting lithium glasses. *Bulletin Mater. Science* **1984**, *6*, 201–221.
- (9) Goodenough, J. B. Ceramic Solid Electrolytes. *Solid State Ionics* **1997**, *94*, 17–25.
- (10) Knauth, P. Inorganic solid Li ion conductors: An overview. *Solid State Ionics* **2009**, *180*, 911–916.
- (11) Banerjee, A.; Wang, X.; Fang, C.; Wu, E. A.; Meng, Y. S. Interfaces and interphases in all-solid-state batteries with inorganic Solid Electrolytes. *Chem. Rev.* **2020**, *120*, 6878–6933.
- (12) Varzi, A.; Raccichini, R.; Passerini, S.; Scrosati, B. J. Challenges and prospects of the role of Solid Electrolytes in the revitalization of lithium metal batteries. *J. Mater. Chem. A* **2016**, *4*, 17251–17259.
- (13) Dixit, M. B.; Zaman, W.; Hortance, N.; Vujic, S.; Harkey, B.; Shen, F.; Tsai, W.-Y.; De Andrade, V.; Chen, X. C.; Balke, N. Nanoscale Mapping of Extrinsic Interfaces in Hybrid Solid Electrolytes. *Joule* **2020**, *4*, 207–221.

- (14) Cheng, X. B.; Zhao, C. Z.; Yao, Y. X.; Liu, H.; Zhang, Q. Recent Advances in Energy Chemistry between Solid-State Electrolyte and Safe Lithium-Metal Anodes. *Chem.* **2019**, *5*, 74–96.
- (15) Famprikis, T.; Canepa, P.; Dawson, J. A.; Islam, M. S.; Masquelier, C. Fundamentals of inorganic solid-state electrolytes for batteries. *Nat. Mater.* **2019**, *18*, 1278.
- (16) Liu, D.; Shadik, Z.; Lin, R.; Qian, K.; Li, H.; Li, K.; Wang, S.; Yu, Q.; Liu, M.; Ganapathy, S.; Qin, X.; Yang, Q. H.; Wagemaker, M.; Kang, F.; Yang, X. Q.; Li, B. Review of Recent Development of In Situ/Operando Characterization Techniques for Lithium Battery Research. *Adv. Mater.* **2019**, *31*, 1806620.
- (17) Cheng, X.-B.; Zhang, R.; Zhao, C.-Z.; Zhang, Q. Toward safe lithium metal anode in rechargeable batteries: a review. *Chem. Rev.* **2017**, *117*, 10403–10473.
- (18) Tippens, J.; Miers, J. C.; Afshar, A.; Lewis, J. A.; Cortes, F. J. Q.; Qiao, H.; Marchese, T. S.; Di Leo, C. V.; Saldana, C.; McDowell, M. T. Visualizing chemomechanical degradation of a solid-state battery electrolyte. *ACS Energy Lett.* **2019**, *4*, 1475–1483.
- (19) Nagao, M.; Hayashi, A.; Tatsumisago, M.; Kanetsuku, T.; Tsuda, T.; Kuwabata, S. In situ SEM study of a lithium deposition and dissolution mechanism in a bulk-type solid-state cell with a $\text{Li}_2\text{S}-\text{P}_2\text{S}_5$ Solid Electrolyte. *Phys. Chem. Chem. Phys.* **2013**, *15*, 18600–18606.
- (20) Liu, X.; Garcia-Mendez, R.; Lupini, A. R.; Cheng, Y.; Hood, Z. D.; Han, F.; Sharafi, A.; Idrobo, J. C.; Dudney, N. J.; Wang, C. Local electronic structure variation resulting in Li 'filament' formation within Solid Electrolytes. *Nat. nanotech* **2021**, *20*, 1485.
- (21) Zhang, L.; Yang, T.; Du, C.; Liu, Q.; Tang, Y.; Zhao, J.; Wang, B.; Chen, T.; Sun, Y.; Jia, P. Lithium whisker growth and stress generation in an in situ atomic force microscope–environmental transmission electron microscope set-up. *Nat. Nanotech* **2020**, *15*, 94–98.
- (22) Pecher, O.; Carretero-Gonzalez, J.; Griffith, K. J.; Grey, C. P. Materials' Methods: NMR in Battery Research. *Chem. Mater.* **2017**, *29*, 213–242.
- (23) Yu, C.; Ganapathy, S.; de Klerk, N. J.; Roslon, I.; van Eck, E. R.; Kentgens, A. P.; Wagemaker, M. Unravelling Li-Ion Transport from Picoseconds to Seconds: Bulk versus Interfaces in an Argyrodite $\text{Li}_6\text{PS}_5\text{Cl}-\text{Li}_2\text{S}$ All-Solid-State Li-Ion Battery. *J. Am. Chem. Soc.* **2016**, *138*, 11192–11201.
- (24) Yu, C.; Ganapathy, S.; Eck, E.; Wang, H.; Basak, S.; Li, Z.; Wagemaker, M. Accessing the bottleneck in all-SSB, lithium-ion transport over the solid-electrolyte-electrode interface. *Nat. Commun.* **2017**, *8*, 1086.
- (25) Ganapathy, S.; van Eck, E. R.; Kentgens, A. P.; Mulder, F. M.; Wagemaker, M. Equilibrium lithium-ion transport between nanocrystalline lithium-inserted anatase TiO_2 and the electrolyte. *Chem.—Eur. J.* **2011**, *17*, 14811–14816.
- (26) Zheng, J.; Tang, M. X.; Hu, Y. Y. Lithium Ion Pathway within $\text{Li}_7\text{La}_3\text{Zr}_2\text{O}_{12}$ -Polyethylene Oxide Composite Electrolytes. *Angew. Chem. Int. Edit* **2016**, *55*, 12538–12542.
- (27) Schwietert, T. K.; Arszewska, V. A.; Wang, C.; Yu, C.; Vasileiadis, A.; de Klerk, N. J. J.; Hageman, J.; Hupfer, T.; Kerkamm, I.; Xu, Y.; van der Maas, E.; Kelder, E. M.; Ganapathy, S.; Wagemaker, M. Clarifying the relationship between redox activity and electrochemical stability in Solid Electrolytes. *Nat. Mater.* **2020**, *19*, 428–435.
- (28) Liu, M.; Wang, C.; Zhao, C.; Maas, E.; Lin, K.; Arszewska, V.; Li, B.; Ganapathy, S.; Wagemaker, M. Quantification of the Li-ion diffusion over an interface coating in all-solid-state batteries via NMR measurements. *Nat. Commun.* **2021**, *12*, 5943.
- (29) Brogioli, D.; Langer, F.; Kun, R.; La Mantia, F. Space-charge effects at the $\text{Li}_7\text{La}_3\text{Zr}_2\text{O}_{12}$ /Poly (ethylene oxide) interface. *ACS Appl. Mater. Inter* **2019**, *11*, 11999–12007.
- (30) Simon, F. J.; Hanauer, M.; Henss, A.; Richter, F. H.; Janek, J. Interfaces. Properties of the interphase formed between argyrodite-type $\text{Li}_6\text{PS}_5\text{Cl}$ and polymer-based PEO_{10} : LiTFSI . *ACS Appl. Mater. Inter* **2019**, *11*, 42186–42196.
- (31) Lei, D.; He, Y. B.; Huang, H.; Yuan, Y.; Zhong, G.; Zhao, Q.; Hao, X.; Zhang, D.; Lai, C.; Zhang, S.; Ma, J.; Wei, Y.; Yu, Q.; Lv, W.; Yu, Y.; Li, B.; Yang, Q.; Yang, Y.; Lu, J.; Kang, F. Cross-linked beta alumina nanowires with compact gel polymer electrolyte coating for ultra-stable sodium metal battery. *Nat. Commun.* **2019**, *10*, 4244.
- (32) Yang, K.; Chen, L.; Ma, J.; Lai, C.; Huang, Y.; Mi, J.; Biao, J.; Zhang, D.; Shi, P.; Xia, H.; Zhong, G.; Kang, F.; He, Y. Stable Interface Chemistry and Multiple Ion Transport of Composite Electrolyte Contribute to Ultra-long Cycling Solid-State $\text{Li}-\text{Ni}_{0.8}\text{Co}_{0.1}\text{Mn}_{0.1}\text{O}_2$ /Lithium Metal Batteries. *Angew. Chem. Int. Edit* **2021**, *60*, 24668–24675.
- (33) Chen, L.; Li, Y. T.; Li, S. P.; Fan, L. Z.; Nan, C. W.; Goodenough, J. B. PEO/garnet composite electrolytes for solid-state lithium batteries: From "ceramic-in-polymer" to "polymer-in-ceramic". *Nano Energy* **2018**, *46*, 176–184.
- (34) Zheng, J.; Wang, P.; Liu, H.; Hu, Y.-Y. Interface-enabled ion conduction in $\text{Li}_{10}\text{GeP}_2\text{S}_{12}$ -poly (ethylene oxide) hybrid electrolytes. *ACS Appl. Energy Mater.* **2019**, *2*, 1452–1459.
- (35) Zaman, W.; Hortance, N.; Dixit, M. B.; De Andrade, V.; Hatzell, K. B. Visualizing percolation and ion transport in hybrid Solid Electrolytes for Li-metal batteries. *J. Mater. Chem. A* **2019**, *7*, 23914–23921.
- (36) Zheng, J.; Hu, Y. Y. New Insights into the Compositional Dependence of Li-Ion Transport in Polymer-Ceramic Composite Electrolytes. *ACS Appl. Mater. Inter* **2018**, *10*, 4113–4120.
- (37) Aurbach, D.; McCloskey, B. D.; Nazar, L. F.; Bruce, P. G. Advances in understanding mechanisms underpinning lithium–air batteries. *Nat. Energy* **2016**, *1*, 16128.
- (38) Bruce, P. G.; Freunberger, S. A.; Hardwick, L. J.; Tarascon, J.-M. $\text{Li}-\text{O}_2$ and $\text{Li}-\text{S}$ batteries with high energy storage. *Nat. Mater.* **2012**, *11*, 19–29.
- (39) Zhang, X.; Wang, A.; Liu, X.; Luo, J. Dendrites in lithium metal anodes: suppression, regulation, and elimination. *Accounts chem research* **2019**, *52*, 3223–3232.
- (40) Shen, F.; Dixit, M. B.; Xiao, X.; Hatzell, K. B. Effect of pore connectivity on Li dendrite propagation within LLZO electrolytes observed with synchrotron X-ray tomography. *ACS Energy Lett.* **2018**, *3*, 1056–1061.
- (41) Porz, L.; Swamy, T.; Sheldon, B. W.; Rettenwander, D.; Frömmling, T.; Thaman, H. L.; Berendts, S.; Uecker, R.; Carter, W. C.; Chiang, Y.-M. Mechanism of lithium metal penetration through inorganic Solid Electrolytes. *Adv. Energy Mater.* **2017**, *7*, 1701003.
- (42) Huo, H. Y.; Chen, Y.; Luo, J.; Yang, X. F.; Guo, X. X.; Sun, X. L. Rational Design of Hierarchical "Ceramic-in-Polymer" and "Polymer-in-Ceramic" Electrolytes for Dendrite-Free Solid-State Batteries. *Adv. Energy Mater.* **2019**, *9*, 1804004.
- (43) Chang, H. J.; Trease, N. M.; Ilott, A. J.; Zeng, D.; Du, L.-S.; Jerschow, A.; Grey, C. P. Investigating Li microstructure formation on Li anodes for lithium batteries by in situ $^6\text{Li}/^7\text{Li}$ NMR and SEM. *J. Phys. Chem. C* **2015**, *119*, 16443–16451.
- (44) Marbella, L. E.; Zekoll, S.; Kasemchainan, J.; Emge, S. P.; Bruce, P. G.; Grey, C. P. ^7Li NMR chemical shift imaging to detect microstructural growth of lithium in all-solid-state batteries. *Chem. Mater.* **2019**, *31*, 2762–2769.
- (45) Bayley, P. M.; Trease, N. M.; Grey, C. P. Insights into electrochemical sodium metal deposition as probed with in situ ^{23}Na NMR. *J. Am. Chem. Soc.* **2016**, *138*, 1955–1961.
- (46) Lv, S.; Verhallen, T.; Vasileiadis, A.; Ooms, F.; Xu, Y.; Li, Z.; Li, Z.; Wagemaker, M. Operando monitoring the lithium spatial distribution of lithium metal anodes. *Nat. Commun.* **2018**, *9*, 2152.
- (47) Tippens, J.; Miers, J. C.; Afshar, A.; Lewis, J. A.; Cortes, F. J. Q.; Qiao, H.; Marchese, T. S.; Di Leo, C. V.; Saldana, C.; McDowell, M. T. Visualizing chemomechanical degradation of a solid-state battery electrolyte. *ACS Energy Lett.* **2019**, *4*, 1475–1483.
- (48) Albertus, P.; Babinec, S.; Litzelman, S.; Newman, A. Status and challenges in enabling the lithium metal electrode for high-energy and low-cost rechargeable batteries. *Nat. Energy* **2018**, *3*, 16–21.
- (49) Kamaya, N.; Homma, K.; Yamakawa, Y.; Hirayama, M.; Kanno, R.; Yonemura, M.; Kamiyama, T.; Kato, Y.; Hama, S.; Kawamoto, K. A lithium superionic conductor. *Nat. Mater.* **2011**, *10*, 682–686.

(50) Zhu, Y.; He, X.; Mo, Y. Origin of outstanding stability in the lithium Solid Electrolyte materials: insights from thermodynamic analyses based on first-principles calculations. *ACS Appl. Mater. Inter* **2015**, *7*, 23685–23693.

(51) Bhattacharyya, R.; Key, B.; Chen, H.; Best, A. S.; Hollenkamp, A. F.; Grey, C. P. In situ NMR observation of the formation of metallic lithium microstructures in lithium batteries. *Nat. Mater.* **2010**, *9*, 504–510.

(52) Liu, M.; Cheng, Z.; Qian, K.; Verhallen, T.; Wang, C.; Wagemaker, M. Efficient Li-Metal Plating/Stripping in Carbonate Electrolytes Using a LiNO₃-Gel Polymer Electrolyte, Monitored by Operando Neutron Depth Profiling. *Chem. Mater.* **2019**, *31*, 4564–4574.

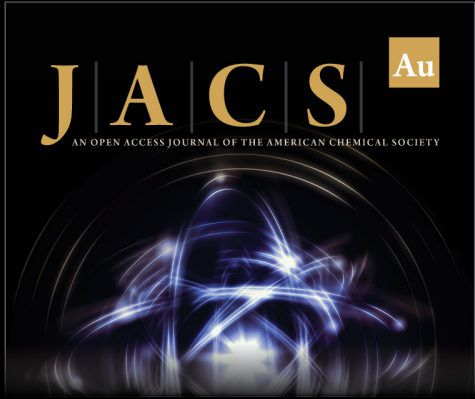
(53) Verhallen, T. W.; Lv, S.; Wagemaker, M. Operando neutron depth profiling to determine the spatial distribution of Li in Li-ion Batteries. *Frontiers in Energy Research* **2018**, *6*, 62.

(54) Wang, C. W.; Gong, Y. H.; Dai, J. Q.; Zhang, L.; Xie, H.; Pastel, G.; Liu, B. Y.; Wachsmann, E.; Wang, H.; Hu, L. B. In Situ Neutron Depth Profiling of Lithium Metal-Garnet Interfaces for SSB. *J. Am. Chem. Soc.* **2017**, *139*, 14257–14264.

(55) Han, F.; Westover, A. S.; Yue, J.; Fan, X.; Wang, F.; Chi, M.; Leonard, D. N.; Dudney, N. J.; Wang, H.; Wang, C. High electronic conductivity as the origin of lithium dendrite formation within Solid Electrolytes. *Nat. Energy* **2019**, *4*, 187–196.

(56) Nagpure, S. C.; Mulligan, P.; Canova, M.; Cao, L. R. Neutron depth profiling of Li-ion cell electrodes with a gas-controlled environment. *J. Power Sources* **2014**, *248*, 489–497.

(57) Trunk, M.; Wetjen, M.; Werner, L.; Gernhauser, R.; Markisch, B.; Revay, Z.; Gasteiger, H. A.; Gilles, R. Materials science applications of Neutron Depth Profiling at the PGAA facility of Heinz Maier-Leibnitz Zentrum. *Mater. Charact* **2018**, *146*, 127–134.



JACS Au
AN OPEN ACCESS JOURNAL OF THE AMERICAN CHEMICAL SOCIETY

 Editor-in-Chief
Prof. Christopher W. Jones
Georgia Institute of Technology, USA

Open for Submissions 

pubs.acs.org/jacsau  ACS Publications
Most Trusted. Most Cited. Most Read.